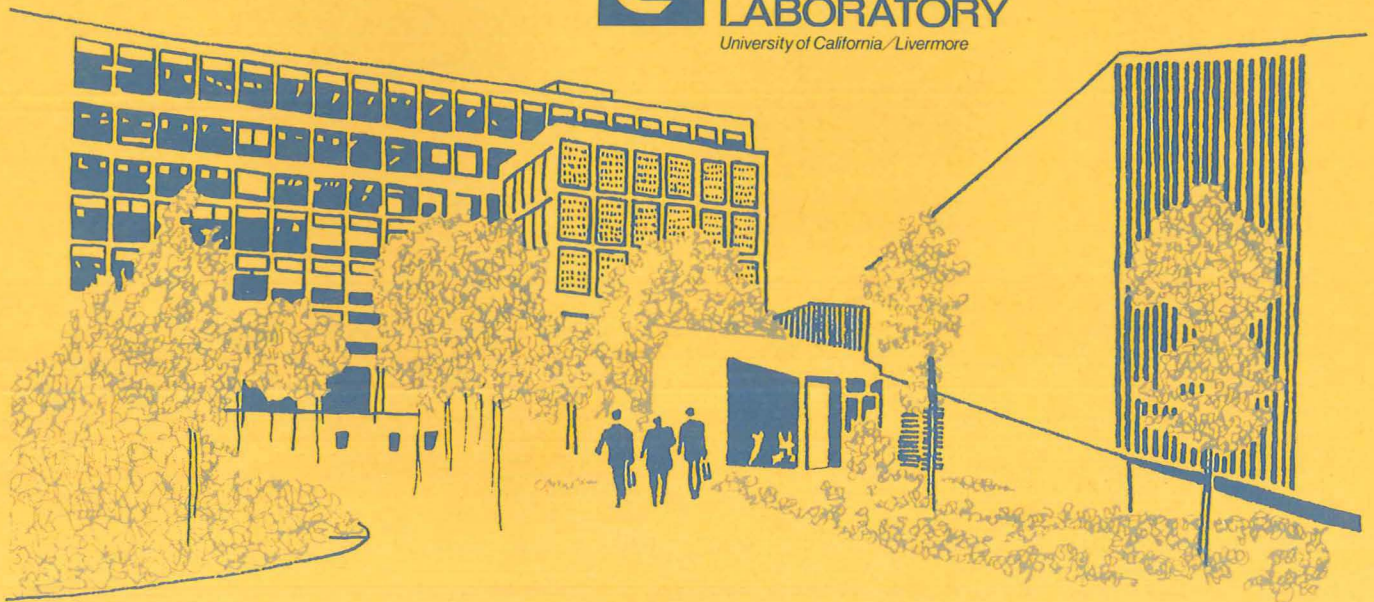


ANALYSIS OF A RADIAL-OUTFLOW REACTION TURBINE CONCEPT FOR GEOTHERMAL APPLICATION

P. A. House

May 25, 1978

Work performed under the auspices of the U.S. Department of
Energy by the UCLLL under contract number W-7405-ENG-48.





LAWRENCE LIVERMORE LABORATORY
University of California / Livermore, California / 94550

UCRL-52480

ANALYSIS OF A RADIAL-OUTFLOW REACTION TURBINE CONCEPT FOR GEOTHERMAL APPLICATION

P. A. House

MS. date: May 25, 1978

NOTICE

"This report was prepared as an account of work sponsored by the United States Government. Neither the United States nor the United States Department of Energy, nor any of their employees, nor any of their contractors, subcontractors, or their employees, makes any warranty, express or implied, or assumes any legal liability or responsibility for the accuracy, completeness or usefulness of any information, apparatus, product or process disclosed, or represents that its use would not infringe privately-owned rights."

NOTICE

Reference to a company or product name does not imply approval or recommendation of the product by the University of California or the U.S. Department of Energy to the exclusion of others that may be suitable.

Printed in the United States of America
Available from
National Technical Information Service
U.S. Department of Commerce
5285 Port Royal Road
Springfield, VA 22161
Price: Printed Copy \$; Microfiche \$3.00

<u>Page Range</u>	<u>Domestic Price</u>	<u>Page Range</u>	<u>Domestic Price</u>
001-025	\$ 4.00	326-350	\$12.00
026-050	4.50	351-375	12.50
051-075	5.25	376-400	13.00
076-100	6.00	401-425	13.25
101-125	6.50	426-450	14.00
126-150	7.25	451-475	14.50
151-175	8.00	476-500	15.00
176-200	9.00	501-525	15.25
201-225	9.25	526-550	15.50
226-250	9.50	551-575	16.25
251-275	10.75	576-600	16.50
276-300	11.00	601-up	¹
301-325	11.75		

¹Add \$2.50 for each additional 100 page increment from 601 pages up.

CONTENTS

Abstract	1
Introduction	1
Radial-Outflow Reaction Turbine	1
Early Pure-Reaction Turbines	1
Motivation for Development	1
Turbine Performance	3
Low-Energy Wellhead Applications	3
High-Energy Wellhead Applications	4
Summary	7
Appendix A: RORT Analysis	8

ANALYSIS OF A RADIAL-OUTFLOW REACTION TURBINE CONCEPT FOR GEOTHERMAL APPLICATION

ABSTRACT

Described herein is the radial-outflow reaction turbine, a pure-reaction turbine designed to improve the conversion efficiency of geothermal energy into electrical power. It also has potential as a total-flow turbine for low-temperature water. We can use the principle of incomplete expansion to obtain a reduction in turbine size when the turbine exhausts into a low-pressure condenser. And, by adding this turbine to single- and two-stage flashed-steam systems, we can improve the conversion efficiency of systems utilizing low- and high-energy wellhead sources, respectively. The Appendix outlines our analysis of the radial-outflow reaction turbine and leads to an expression for engine efficiency.

INTRODUCTION

Nonconventional conversion technology is needed to obtain efficient power generation from a liquid-dominated geothermal reservoir. One nonconventional conversion device, the pure-reaction turbine, is designed to produce power from the ex-

pansion of saturated water. This report is an analysis of one pure-reaction turbine—the radial-outflow reaction turbine—and its geothermal application.

RADIAL-OUTFLOW REACTION TURBINE

At Lawrence Livermore Laboratory (LLL), we are evaluating and testing an experimental radial-outflow reaction turbine (RORT) with a 16-in.-diam rotor. Figure 1 shows the RORT configuration. Here hot water is conducted radially out to revolving liquid and two-phase steam nozzles. The energy added to the liquid in the revolving ducts as increased head and velocity is partially recovered in the liquid nozzles. The thermal energy is then utilized by means of thrust developed in the steam nozzles.

Barker's Mill (Fig. 3) was used to produce mechanical power from a change in stream or river elevation. The device consisted of a hydraulic reaction turbine where power was developed by revolving liquid nozzles. The RORT differs from these early predecessors by virtue of two-phase expansion in the revolving nozzles.

Early Pure-Reaction Turbines

The RORT combines the features of two early pure-reaction turbines—Hero's reaction turbine and "Barker's Mill." Hero's reaction turbine (120 B.C.) was essentially a vapor turbine wherein saturated vapor was fed to ducts leading to revolving vapor nozzles (Fig. 2). A device employed in

Motivation for Development

Our motivations for developing the RORT were to enhance the performance of one- and two-stage flashed-steam systems and the need for a total-flow turbine for low-temperature ($\leq 350^\circ\text{F}$) water. We selected the reaction turbine for saturated water rather than the impulse turbine because of its simplicity, relatively high realizable efficiency, and freedom from blade erosion problems.

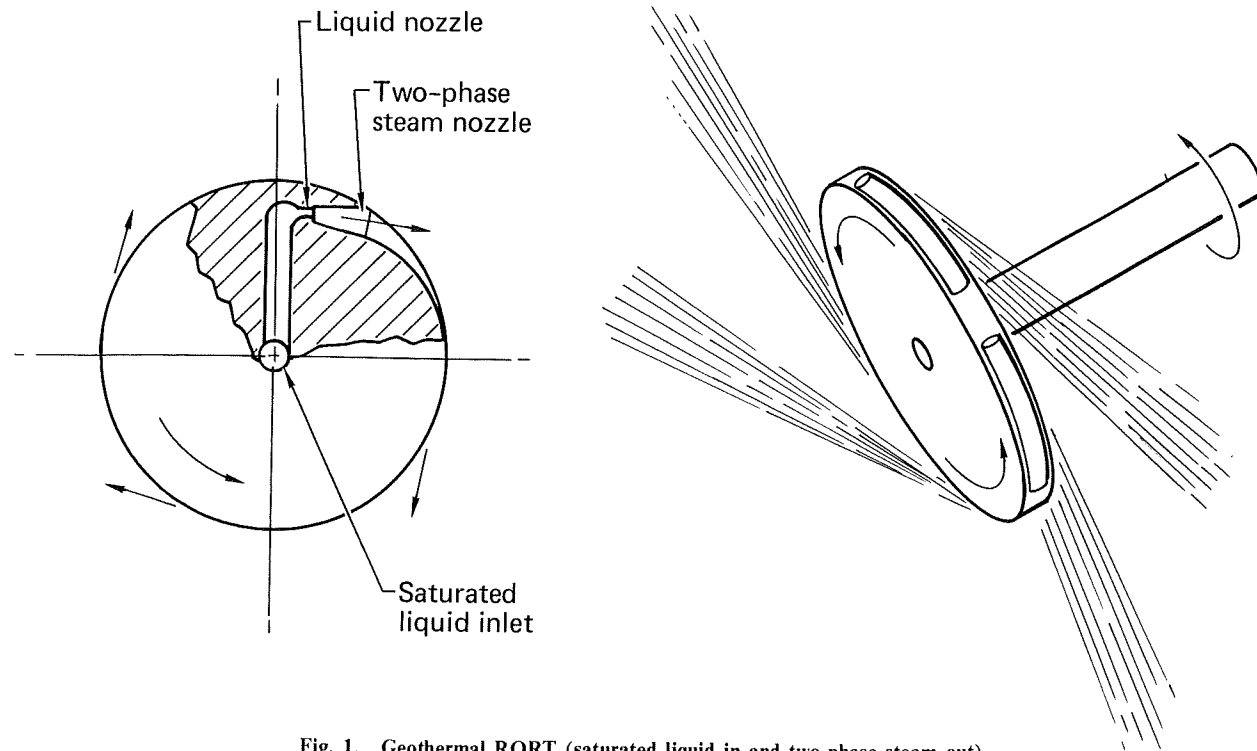


Fig. 1. Geothermal RORT (saturated liquid in and two-phase steam out).

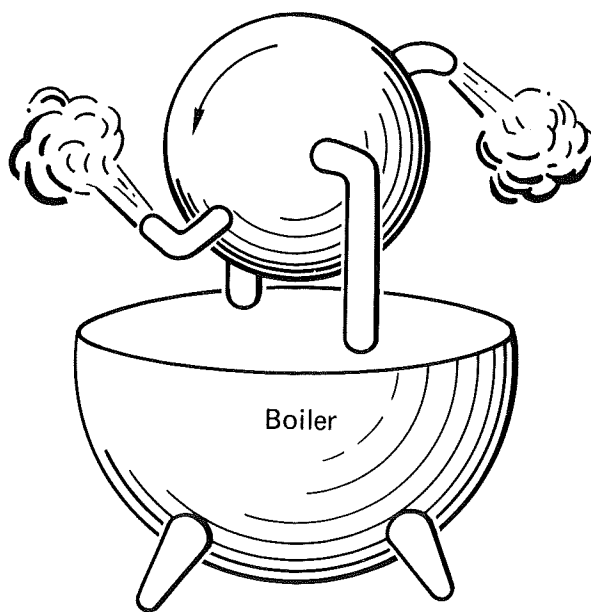


Fig. 2. Hero's reaction turbine (all vapor).

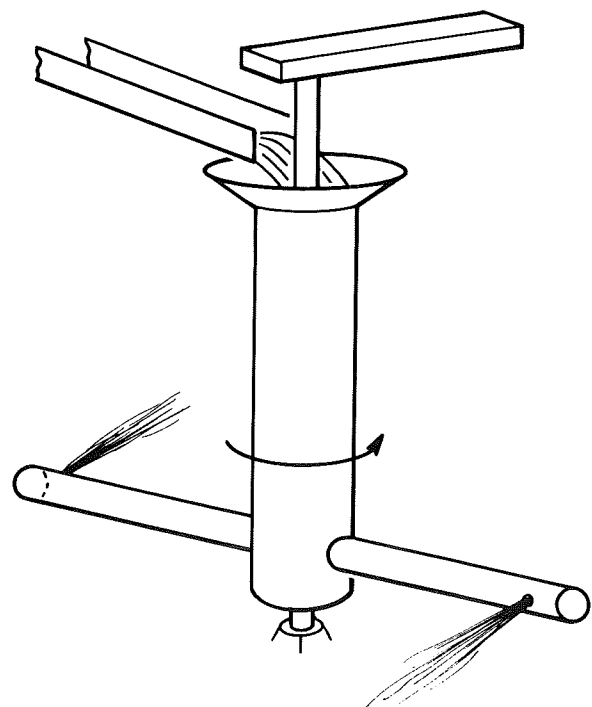


Fig. 3. Barker's Mill (all liquid).

TURBINE PERFORMANCE

In the Appendix, we analyze the RORT and derive an expression for engine efficiency. Calculated engine efficiency is essentially independent of turbine size and the magnitude of available energy. From a practical standpoint, however, disk stresses will probably limit turbine use to those expansions where the isentropic enthalpy drop is no more than about 40 Btu/lb. This would allow a RORT with a 120°F condenser to function as a total-flow turbine for saturated water at temperatures up to 350°F. When the RORT is used in conjunction with conventional vapor turbines in a hybrid system, however, the whole range of wellhead energies may be utilized.

Figure 4 shows engine efficiency as a function of angular velocity and the liquid-capture factor α . Although engine efficiencies of 40% to 50% appear feasible, we will have to do some experimental work to determine whether the assumed nozzle efficiencies, liquid capture on the steam nozzle walls (4% to 10%), and slip between phases are reasonable. Our first step will be to measure the performance of an experimental nozzle designed to simulate the revolving nozzle condition of high (compressed liquid) initial pressure.

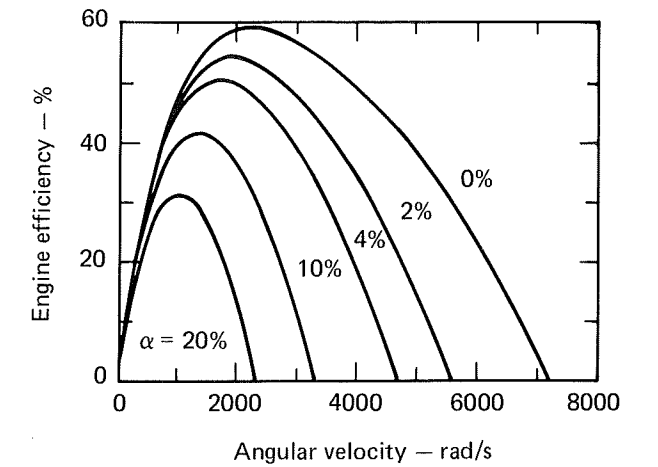


Fig. 4. RORT engine efficiencies as a function of angular velocity and the liquid capture factor, α . This RORT had a 16-in.-diam rotor; a 350-psia saturated liquid inlet; a 20-psia exhaust (20% quality); a 60% slip; 95% liquid and 75% two-phase steam nozzle efficiencies; and 8° steam and 4° liquid discharge angles.

LOW-ENERGY WELLHEAD APPLICATIONS

One application of the RORT is for saturated water at the wellhead. In this application, the RORT may be used as a total-flow expander or in a simple advanced flash-steam or hybrid system. When it is used as a total-flow expander, the principle of incomplete expansion (Fig. 5) can reduce turbine size; some loss in engine efficiency would also be experienced.

In normal operation (complete expansion), nozzle exit pressure (P_1) is equal to turbine case pressure (P_2). Increased turbine power output may be gained by lowering P_2 without increasing turbine size. This increased power results from an unbalanced force in the direction of motion, the force being equal to $(P_1 - P_2)$ multiplied by the area of the nozzle exit plane. The question of how much incomplete expansion to use would be based on economics. Although quantification of potential size reduction vs loss in engine efficiency will be the subject of a future study, preliminary results indicate the expander size for a 120°F condenser may be reduced by more than a factor of 2 with less than a 5% reduction in engine efficiency.

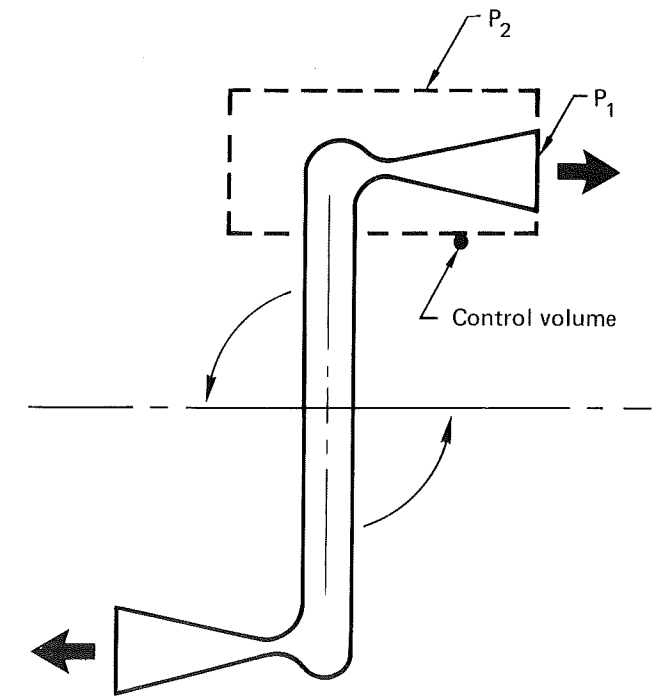


Fig. 5. Incomplete expansion.

In Fig. 6, we compare two methods of using the RORT—total flow and a hybrid system—with one- and two-stage flashed-steam systems. The systems have, in each case, been optimized to maximize engine efficiency. Figure 6 also shows assumed pressure drops in the separator/scrubber system. At an assumed RORT efficiency of 40%, the single-

stage flashed-steam system has a slight edge over the total-flow turbine. If RORT efficiency were increased to 50%, the total-flow turbine would have the advantage. However, the RORT is better applied in the hybrid system where, with less equipment, it outperforms the two-stage flashed-steam system.

HIGH-ENERGY WELLHEAD APPLICATIONS

One excellent application for the RORT is in the advanced flashed-steam system (Fig. 7) where it is used to expand liquid from the high- to the low-pressure separator. Vapor turbines are indicated by T1 and T2. Since the exhaust from T1 and from the RORT is "dried out" in the second separator before going to the scrubber and T2, there is only one low-pressure turbine in the system and vapor turbine (T1 and T2) exhaust moisture is held to low values.

We calculated optimized system performance for three assumed RORT efficiencies (0, 40, and 60%) and four representative self-pumping wellhead conditions.* A RORT efficiency of 0% means it has been replaced by a throttling device and the system is, for the purposes of comparison, a two-stage flashed-steam system. These wellhead conditions,

together with system pressure and pressure-drop constraints, are listed in Table 1. In all cases, we assumed vapor turbine efficiencies of 70%.

We assigned a minimum difference of $P_1 - P_2$ max between P_1 and P_2 to account for some pressure loss in the wellhead-gathering piping. Deliberate throttling from the wellhead state was only desirable for the flashed-steam system (reaction turbine not present).

The results of our calculations are shown in Table 2. We obtained effective engine efficiency by dividing the isentropic work into the sum of the turbine work (per pound of wellhead fluid). When we compared the advanced system to the conventional system, we noted an average potential increase of about 17% for a 60%-efficient RORT.

We also found a RORT with about a 40% engine efficiency contributes approximately 12% to 15% of the total work, with slightly over half the work being accomplished in the low-pressure turbine (T2). The effective engine efficiency results are shown in Fig. 8 as a function of reservoir temperature.

*A. L. Austin, *Prospects for Advances in Energy Conversion Technologies for Geothermal Energy Development*, Lawrence Livermore Laboratory, Rept. UCRL-76532 (1975).

Table 1. Wellhead conditions and system pressure and pressure-drop constraints for four types of reservoirs.

Reservoir Type	Wellhead			System ^a			
	Temperature (°F)	Pressure (psia)	Quality	P_2 max (psia)	$P_2 - P_{22}$ (psia)	P_5 min (psia)	$P_5 - P_{55}$ (psia)
I	350	50	0.07371	48	2	8	0.5
II	400	98	0.08328	94	2	10	0.5
III	500	220	0.1372	214	2	14	1
IV	572	360	0.1890	352	2	16	1

^aNumbers indicate system pressures. See Fig. 7.

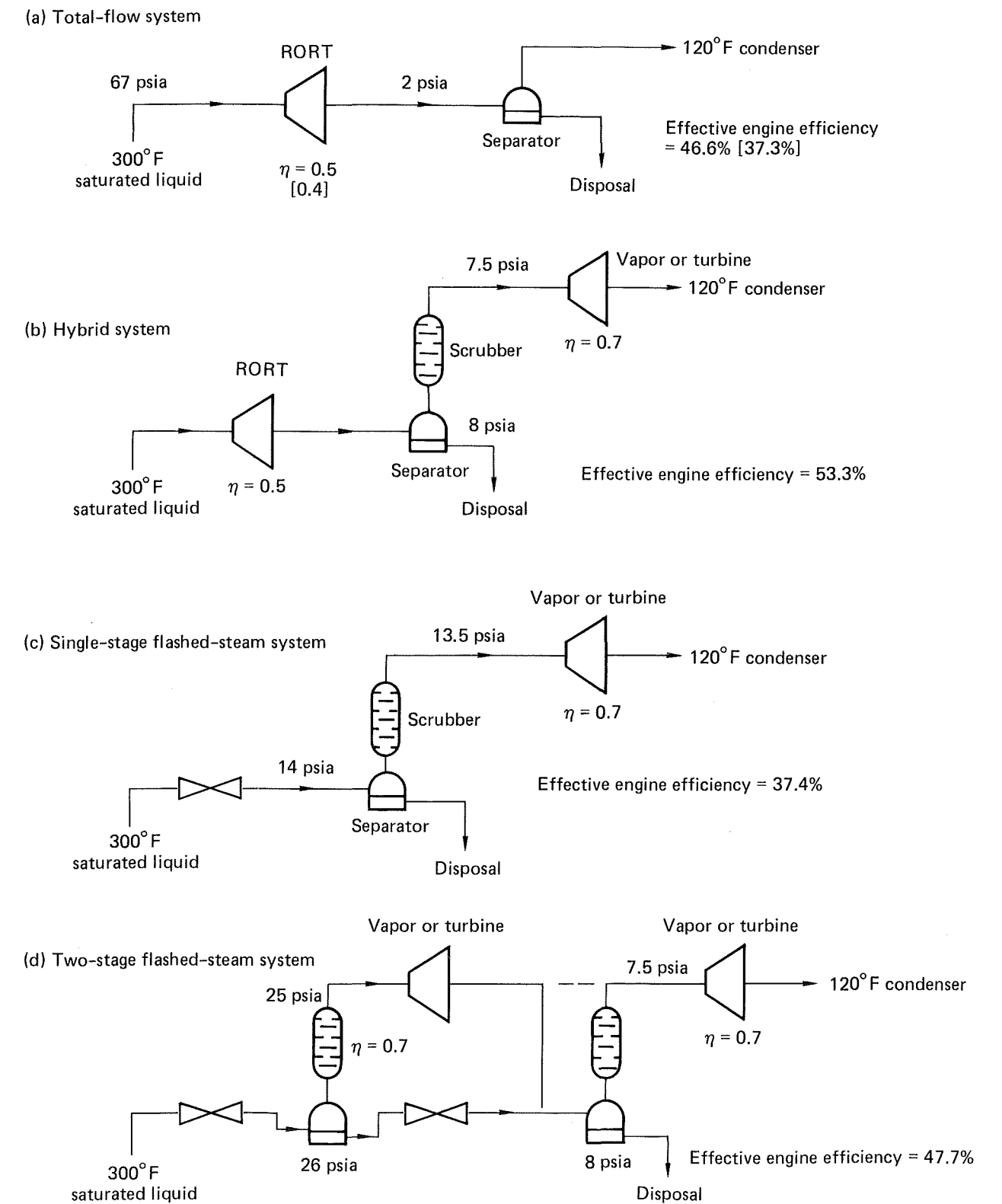


Fig. 6. Systems for saturated liquid expansion.

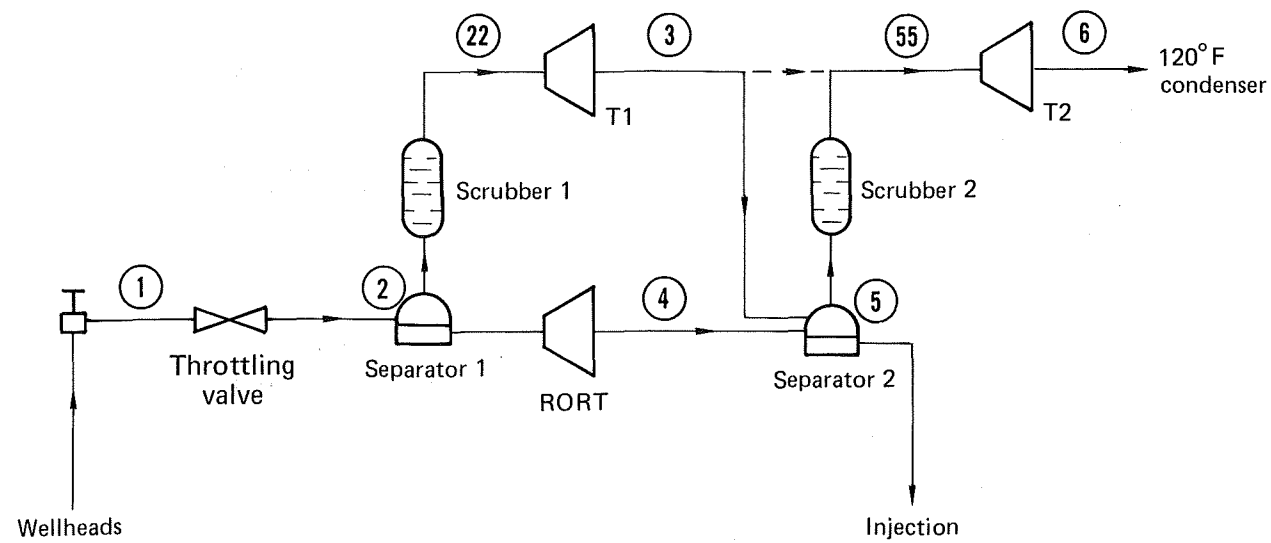


Fig. 7. Advanced flashed-steam system.

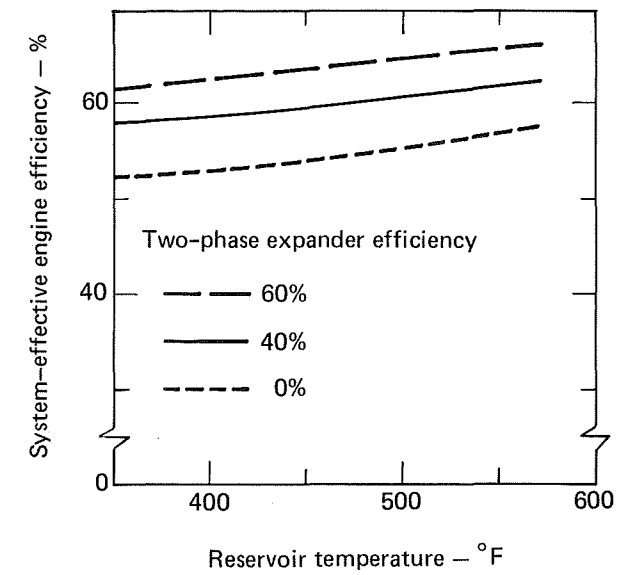


Fig. 8. Effective engine efficiency results for an advanced flash-steam system as a function of reservoir temperature. This system had 70% vapor turbines; a 120°F condenser; and 2-psia high-pressure and 0.5- to 1-psia low-pressure separator pressure losses.

Table 2. Calculated performance of advanced flashed-steam system.^a

P_2 (psia)	P_{22} (psia)	P_5 (psia)	P_{55} (psia)	X_3	X_4	X_6	DHT1	DHRT	DHT2	EF	EE
Reservoir I. Isentropic enthalpy change = 34.098 Btu/lb.											
48	46	8	7.5	0.9461	0.09379	0.9587	6.597	3.708	10.637	0.6	61.42
48	46	8	7.5	0.9461	0.09515	0.9587	6.597	2.472	10.721	0.4	58.04
44	42	11	10.5	0.9573	0.07786	0.9496	5.523	0	12.338	0	52.38
Reservoir II. Isentropic enthalpy change = 50.124 Btu/lb.											
94	92	10	9.5	0.9299	0.1277	0.9523	9.603	6.577	15.321	0.6	62.84
94	92	10	9.5	0.9299	0.1302	0.9523	9.603	4.385	15.494	0.4	58.82
72	70	15	14.5	0.9492	0.0964	0.9411	8.391	0	18.155	0	52.96
Reservoir III. Isentropic enthalpy change = 86.937 Btu/lb.											
214	212	14	13	0.9092	0.1759	0.9440	19.264	11.150	25.633	0.6	64.47
214	212	16	15	0.9122	0.1748	0.9402	18.453	6.879	27.404	0.4	60.66
168	166	26	25	0.9333	0.1362	0.9268	15.804	0	32.385	0	55.43
Reservoir IV. Isentropic enthalpy change = 119.703 Btu/lb.											
352	350	16	15	0.8923	0.2141	0.9402	29.863	15.153	33.915	0.6	65.94
352	350	21	20	0.8980	0.2094	0.9326	27.633	8.818	38.146	0.4	62.32
292	290	38	37	0.9204	0.1692	0.9166	22.828	0	45.900	0	57.42

^aP = pressure; X = quality; DH = enthalpy change per pound of wellhead fluid; T1 and T2 = vapor turbines; RT = RORT; EF = RORT efficiency; and EE = engine efficiency.

SUMMARY

The RORT is a versatile means of converting geothermal energy into electrical power. Its inherent simplicity and ruggedness make it a natural choice for the expansion of geothermal brine, and it offers

potential as a total-flow turbine for low-temperature water. Before we can realize the RORT's full potential, however, we will need a development program.

APPENDIX A: RORT ANALYSIS

This Appendix outlines our analysis of RORT performance and leads to an expression of engine efficiency.

Work Added to the Liquid in the Ducts

The velocity at the nozzle entrance was equal to

$$\frac{r_n \omega}{12} = U_n,$$

where

r = radius (in.) at the centerline of the nozzle entrance

ω = angular velocity (rad/s)

U_n = velocity (fps)

and the work due to the velocity

$$\equiv W_u = \frac{U_n^2}{2g} = \frac{r_n^2 \omega^2}{288g} \text{ in ft-lb}_f/\text{lb}_m.$$

The head at the nozzle entrance due to rotation is illustrated in Fig. A1. From Fig. A1, we see the liquid mass, $ma = \gamma Ar_n/12g$, slugs

$$\bullet \text{ Force (F)} = ma = \frac{\gamma Ar_n}{12g} \left[\frac{r_n \omega^2}{12(2)} \right] = \frac{\gamma Ar_n^2 \omega^2}{288g}$$

$$\bullet \text{ Pressure (P)} = F/A = \frac{\gamma r_n^2 \omega^2}{288g}$$

$$\bullet \text{ Head (H)} = \frac{P}{\gamma} = \frac{r_n^2 \omega^2}{288g} \text{ in ft-lb}_f/\text{lb}_m$$

where

γ = specific weight (lb/ft³)

A = area (ft²)

r_n = radius (in.)

$$g = 32.2 \left(\frac{\text{lb}_m/\text{ft}}{\text{lb}/\text{s}^2} \right)$$

The total work added to the liquid (W_a) was equal to

$$W_u + H = \frac{r_n^2 \omega^2}{144g} \quad (1)$$

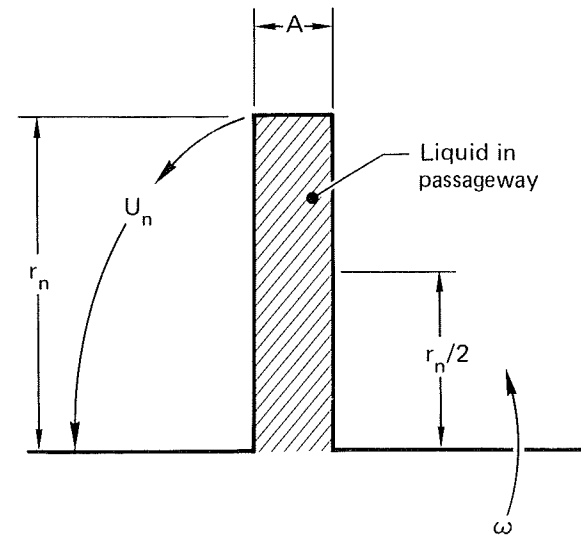


Fig. A1. Model for determining the liquid head.

Work Recovered from the Liquid

We recovered part of the work in the liquid nozzles by means of the revolving thrust vector

$$F_t = \frac{Q\gamma V_1}{g},$$

where

F_t = force from the nozzle reaction

Q = flowrate (ft³/s)

V_1 = liquid velocity (fps)

To minimize the number of liquid droplets that hit the nozzle wall during steam expansion, we considered discharge angles θ and β for the liquid and two-phase expansions, respectively. See Fig. A2.

We found work equal to

$$F_t \cos \theta \left(\frac{2\pi r_n}{12} \right) \text{ in ft-lb}_f/\text{revolution}$$

and power equal to

$$\frac{W\omega}{2\pi} = \frac{F_t \cos \theta 2\pi r_n \omega}{12 (2\pi)} \text{ in ft-lb}_f/\text{s}.$$

However, $Q = \dot{m}/\gamma$; therefore, power was equal to

$$\frac{\dot{m} V_1 \cos \theta (r_n \omega)}{12g} \text{ in ft-lb}_f/\text{s}.$$

The work recovered (W_r) was equal to power/ \dot{m} ; therefore, it was equal to

$$\frac{r_n \omega V_1 \cos \theta}{12g} \text{ in ft-lb}_f/\text{lb}_m.$$

However, $V_1 = \sqrt{2g H \eta_f}$, where η_f was equal to the liquid nozzle efficiency, but

$$H = \frac{r_n^2 \omega^2}{(12)^2 (2)g}.$$

The liquid nozzle discharge velocity (V_1) was equal to

$$\frac{r_n \omega}{12} \sqrt{\eta_f}, \quad (2)$$

and the work recovered from the liquid was equal to

$$\frac{r_n \omega (r_n \omega) \sqrt{\eta_f} \cos \theta}{12(12)g} = \frac{r_n^2 \omega^2 \sqrt{\eta_f} \cos \theta}{144g} \quad (3)$$

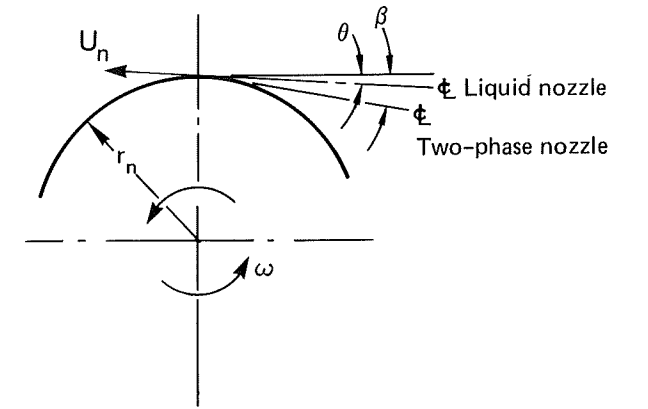


Fig. A2. Nozzle angles.

Thus, the net amount of work lost, $W_f = W_r - W_a$, was equal to

$$u = \frac{r_n^2 \omega^2 \sqrt{\eta_f} \cos \theta}{144g} - \frac{r_n^2 \omega^2}{144g} \text{ in ft-lb}_f/\text{lb}_m,$$

and the work lost (W_f) due to the inefficiency and discharge angle of the liquid nozzle was equal to

$$\frac{-r_n^2 \omega^2}{144Jg} (1 - \cos \theta \sqrt{\eta_f}) \text{ in Btu/lb}_m. \quad (4)$$

Work Added from Thermal Energy

Using the initial velocity, $V_1 = \frac{r_n \omega}{12} \sqrt{\eta_f}$, we found the effective final velocity of the combined phases (V_n), which was equal to

$$\sqrt{2Jg\Delta h_s \eta_n + V_1^2} \text{ in fps},$$

where

Δh_s = isentropic enthalpy change (Btu/lb_m)

η_n = two-phase steam nozzle efficiency

The effective combined phase relative to the nozzle exit velocity

$$V_n = \sqrt{2Jg\Delta h_s \eta_n + \frac{r_n^2 \omega^2 \eta_f}{144}}. \quad (5)$$

Slip

Slip (ϵ) is the gain in liquid velocity divided by the gain in vapor velocity or

$$\epsilon = \frac{V_f - V_1}{V_g - V_1}. \quad (6)$$

From Eq. (6), we obtained the droplet velocity

$$V_f = V_1 + \epsilon(V_g - V_1). \quad (7)$$

And, from conservation of energy,

$$V_n^2 = X_r V_g^2 + (1 - X_r) V_f^2, \quad (8)$$

where

$$X_r = \text{quality based on mass-flow-rate ratio} = \left(\frac{\dot{m}_g}{\dot{m}_g + \dot{m}_f} \right)$$

V_g = vapor velocity (fps)

V_f = liquid droplet velocity (fps)

Using Eqs. (7) and (8), we solved the vapor velocity,

$$V_g = \frac{-b + \sqrt{b^2 - 4ac}}{2a}, \quad (9)$$

where

$$a = X_r + (1 - X_r)\epsilon^2$$

$$b = (1 - X_r)(2V_1)(\epsilon - \epsilon^2)$$

$$c = (1 - X_r)(1 - 2\epsilon + \epsilon^2)V_1^2 - V_n^2$$

Once we found the vapor velocity from Eq. (9), we were able to find the liquid droplet velocity from Eq. (7).

Nozzle Thrust

The force from the vapor (F_g) was equal to

$$\frac{\dot{m}_g}{g}(V_g - V_1) = \frac{X_r \dot{m}}{g}(V_g - V_1),$$

and that from the droplets (F_f) was equal to

$$\frac{\dot{m}_f}{g}(V_f - V_1) = \frac{(1 - X_r)\dot{m}}{g}(V_f - V_1).$$

Combining the forces

$$\sum F = F_g + F_f = \frac{\dot{m}}{g} [X_r(V_g - V_1) + (1 - X_r)(V_f - V_1)]$$

gave us the component of force in the direction of motion

$$W_t = \frac{\left(\sum F \cos \beta \right) r_n \omega}{12J\dot{m}} \text{ in Btu/lb}_m$$

and the work obtained from the thermal energy

$$W_t = \frac{r_n \omega \cos \beta}{12Jg} [X_r(V_g - V_1) + (1 - X_r)(V_f - V_1)] \text{ in Btu/lb}_m. \quad (10)$$

Work Lost from Capture of Liquid Droplets on the Nozzle Wall

We let α equal the mass portion of liquid that hit the steam nozzle wall. The worst assumption we could make was that the droplets hit the nozzle wall at their final velocity (V_f) and were slowed to zero relative velocity at the turbine disk radius (r_d). The force due to deceleration of a portion of the droplets was

$$F_d = \frac{\alpha \dot{m}(1 - X_r)V_f}{g}.$$

The work lost (W_d) due to deceleration of liquid droplets in the steam nozzles was equal to

$$\frac{-F_d r_d \omega}{12 J \dot{m}} = \frac{-\alpha \dot{m} (1 - X_r) V_f r_d \omega}{12 J \dot{m}} = \frac{-\alpha (1 - X_r) V_f r_d \omega}{12 J g} \quad (11)$$

Engine Efficiency

Engine efficiency (η_e) was equal to the net work divided by the isentropic enthalpy change (from a saturated liquid expansion to turbine case pressure).

$$\eta_e = \frac{W_t + W_f + W_d}{\Delta h_s} \quad (12)$$

We determined engine efficiency from Eqs. (4), (10), (11), and (12) to be

$$\eta_e = \frac{r_n \omega}{12 J g \Delta h_s} \left\{ \left[X_r (V_g - V_1) + (1 - X_r) (V_f - V_1) \right] \cos \beta - \frac{r_n \omega}{12} (1 - \sqrt{n_r} \cos \theta) - \frac{\alpha (1 - X_r) V_f r_d}{r_n} \right\} \quad (13)$$

using the following equations to find η_e :

Term	Equation	Unit
V_1	(2)	fps
$V_g (V_n)$	(9) [5]	fps
V_f	(7)	fps

To solve the equations, we needed the parameters in Table A1.

Results

Our analysis of the RORT showed us that when ideal assumptions are made ($\eta_f = \eta_n = \epsilon = 1$ and $\theta = \beta = \alpha = 0$), engine efficiency will approach 100% as ω approaches infinity. For more realistic assumptions, the efficiency will peak out at finite values of ω (Fig. 4). We expect, based on preliminary checks, that disk and bearing friction will have a relatively small effect on these results.

We also found that the droplet capture factor (α) has a powerful influence on engine efficiency. Therefore, we added a step between the liquid nozzle exit and the steam nozzle inlet (Fig. 1) to initially keep the high-velocity liquid stream off the steam nozzle wall. We can expect liquid nozzle inlet pressures [Eq. (14)] to be high, e.g. 4570 psi at 1500 rad/s for the rotor shown in Fig. 4.

$$P_n = \frac{r_n^2 \omega^2 \gamma}{2g(12)^4} \text{ psi} \quad (14)$$

Table A1. Turbine performance parameters.

Parameter	How obtained	Unit
r_n	Radius to the centerline of the liquid nozzle exit plane	in.
r_d	Turbine disk radius	in.
ω	Angular disk velocity	rad/s
θ	Liquid nozzle discharge angle	degrees
β	Steam nozzle discharge angle	degrees
η_f	Estimated liquid nozzle efficiency	-
η_n	Estimated or measured steam nozzle efficiency	-
X_r	Quality of the steam nozzle exit plane calculated from the initial temperature of the saturated liquid, from the discharge pressure, and from the efficiency term (η_n), based on $\left(\frac{\dot{m}_g}{\dot{m}_g + \dot{m}_f} \right)$	-
ϵ	Estimated or calculated slip $\left(\frac{V_f - V_1}{V_g - V_1} \right)$	-
α	Liquid droplet capture factor (estimated until indirect data are available)	-
Δh_s	Isentropic enthalpy change due to ideal expansion from the saturated liquid line to the nozzle discharge pressure.	Btu/lb _m

Technical Information Department
LAWRENCE LIVERMORE LABORATORY
University of California | Livermore, California | 94550



THIRD CLASS